International Journal of Engineering and Advanced Technology (IJEAT)
ISSN: 2249-8958 (Online), Volume-4 Issue-4, April 2015

# Modeling and Simulation of Industrial SCARA Robot Arm

**Yousif Ismail Mohammed, Safwan Mawlood Hussein**

***Abstract:*** ***Many industrial applications needed inelegant robot, especially with trajectory processing for movement and pressing things with very accurate points. This paper presents study of Adaptive Neuro Fuzzy Inference Scheme (ANFIS) for Selective Compliant Assembly Robot. Detail description of a Four degrees of freedom (DOFs) mathematical model of an industrial-application SCARA robot with three (shoulder, elbow, wrist) controlled by servo motors and one pneumatics. DC servomotor driving each of the robot-arm joint is modeled and analytical inverse kinematic problem (IKP) and the forward kinematic solution by D-H parameters. Neural networks with fuzzy logic controller (FLC) select the proper rule base through the RBFNN algorithm as inelegant controller for driving the robot with specific trajectory and apply specific handling processing suitable with certain job. The simulation of mathematical model is done by using Matlab Ver. 2014a, satisfactory results was obtained proved the implement of the system design as practical implement with accurate industrial application.***

***Keywords: SCARA robot, Adaptive Neuro Fuzzy Inference Strategy (ANFIS), Industrial applications***

## I. INTRODUCTION

SCARA manipulators frequently perform tasks such as defect removal, pick-and-place, brushing, hole pegging, circuit board assembly, and mechanical assembly, all which require accurate tracking and high-speed maneuvering of the end-effector. Conventional high-speed robots cannot handle large payloads (10kg-20kg), whereas robots handling large payloads cannot reach high speeds. Servo hydraulics makes high speeds and payloads possible. Parallel kinematic mechanisms with stationary actuators often produce the high speeds [1]. Sometimes, the haste can reach a point that could be much faster than gravitational acceleration for instance some can reach haste up to 785 $ms^{-2}$ which is about eighty times faster than gravitational speed. Unfortunately, this speed cannot be used because of the limitation and suitability of the operating envelopes. To remedy the difficulty of inactivity, belt drive system and other components from moving parts such as power transmission and actuator On other hand defines reactions and friction is another difficulty of the system, many studies has been conducted in this area. Toumi and Kuo proposed the using of fast load conveyance (FALCON) robot and direct drive manipulator (DoF MIT). The tracking speed of their project it can reach 3 m/s, which its accuracy between 0.05 and 0.1 mm and its acceleration equal to 3.8 of the gravitational acceleration.

**Manuscript published on 30 April 2015.**
***** Correspondence Author (s)
**Yousif Ismail Mohammed**, Department of Computer Engineering– Engineering College – Ishik University, Erbil, Iraq.
**Safwan Mawlood Hussein**, Department of Computer Engineering– Engineering College – Ishik University, Erbil, Iraq.



Hydraulic cab be used as a solution of high- payload and high speed problem[2-5]. In addition, vibration could be one of the difficulties.

Selective Compliance Assembly Robot Arm is widely used by planar operations. The brushless DC motors leads SCARA manipulator traditional commercial, it can generate huge torques but still indicate to system inertia. To remedy this issue, revolute joints coupled by gears or belt drives are used, In addition to this, the solution introduces these issues such as friction, delay and slip. Which indicate handling electric-motor-driven SCARA turn out to be in applicable of using haste, and large-pay load [6-10].

This paper contains introduction, mathematical model for SCARA robot, design of Adaptive Neuro Fuzzy Inference Scheme controller, SCARA robot Virtual Reality with industrial application and simulation results for system design with conclusion.

## II. MATHEMATICAL MODEL FOR SCARA ROBOT

### 2.1 Inverse Kinematics

Table 1 defines the Denavit-Hartenberg (D-H) parameters specifying the robot arm.

**Table1: The robot D-H parameters**

| $i$ | $d_i$ | $\theta i$ | $a_i$ | $\alpha_i$ |
|---|---|---|---|---|
| 1 | 0 | $\theta_1$ | $L_1$ | 0 |
| 2 | 0 | $\theta_2$ | $L_2$ | 0 |
| 3 | $d_3$ | 0 | 0 | 0 |
| 4 | $d_4$ | $\theta_4$ | 0 | 0 |

By using Table.1[11], then the transformation matrices will be as follows:

$$T_1^0 = B_1 = \begin{bmatrix} c_1 & s_1 & 0 & L \\ -s_1 & c_1 & 0 & L_1 c_1 \\ 0 & 0 & 1 & 0 \\ 0 & 0 & 0 & 1 \end{bmatrix} \quad (1)$$


*Published By:*
*Blue Eyes Intelligence Engineering and Sciences Publication (BEIESP)*

$$T_2^1 = B_2 = \begin{bmatrix} c_2 & s_2 & 0 & L_2 s_2 \\ -s_2 & c_2 & 0 & L_2 c_2 \\ 0 & 0 & 1 & 0 \\ 0 & 0 & 0 & 1 \end{bmatrix} \quad (2)$$

$$T_3^2 = B_3 = \begin{bmatrix} 1 & 0 & 0 & 0 \\ 0 & 1 & 0 & 0 \\ 0 & 0 & 1 & -d_3 \\ 0 & 0 & 0 & 1 \end{bmatrix} \quad (3)$$

$$T_4^3 = B_4 = \begin{bmatrix} c_4 & s_4 & 0 & 0 \\ -s_4 & c_4 & 0 & 0 \\ 0 & 0 & 1 & -d_4 \\ 0 & 0 & 0 & 1 \end{bmatrix} \quad (4)$$

Finally, total transformation matrix will as below:

$$T_4^0 = \begin{bmatrix} c_{124} & s_{124} & 0 & L_2 s_1 + L_1 s_1 \\ -s_{124} & c_{124} & 0 & L_2 c_{12} + L_1 c_1 \\ 0 & 0 & 1 & -d_3 - d_4 \\ 0 & 0 & 0 & 1 \end{bmatrix} \quad (5)$$

**a) Position Inverse**

The SCARA robot desired location is:-

$$T_H^R = \begin{bmatrix} n_x & o_x & a_x & p_x \\ n_y & o_y & a_y & p_y \\ n_z & o_z & a_z & p_z \\ 0 & 0 & 0 & 1 \end{bmatrix} \quad (6)$$

The following equations present the robot [12-19]:

$$T_H^R = B_1 B_2 B_3 B_4 = T_4^0 \quad (7)$$

To determined *B*4 by subtract Eq.1,2, 3, and eq.6 into using eq. (7), such that:

$$B_3^{-1} B_2^{-1} B_1^{-1} T_H^R = B_4 \quad (8)$$

$$\begin{bmatrix} n_x c_{12} + n_y s_{12} & o_x c_{12} + o_y s_{12} & a_x c_{12} + a_y s_{12} & p_x c_{12} + p_y s_{12} - L_1 c_2 - L_2 \\ -n_x s_{12} + n_y c_{12} & o_x s_{12} + o_y c_{12} & -a_x s_{12} + a_y c_{12} & -p_x s_{12} + p_y c_{12} - L_1 s_2 \\ n_z & o_z & a_z & p_z + d_3 \\ 0 & 0 & 0 & 1 \end{bmatrix} = B_4$$

By comparing Eq.(4) and Eq.(8)

$$p_x = L_1 s_1 + L_2 s_{12} \quad (9)$$

$$p_y = L_1 c_1 + L_2 c_{12} \quad (10)$$

And from equation 9 and equation 10,

$$s_2 = \frac{1}{2L_1 L_2}\left(p_x^2 + p_y^2 - L_1^2 - L_2^2\right) \quad (11)$$

$$c_2 = \pm\sqrt{1 - s_2^2} \quad (12)$$

$$\theta_2 = \tan^{-1}\frac{c_2}{s_2} \quad (13)$$

Then rewrite equation (9) and equation (10) as follows:

$$p_x = \left(L_1 + L_2 s_2\right)s_1 - L_2 c_2 c_1 \quad (14)$$

$$p_y = L_2 c_2 s_1 + \left(L_1 + L_2 s_2\right)c_1 \quad (15)$$

By kramer's rule to solving equations (14) and (15):

$$\Delta = \begin{bmatrix} L_1 + L_2 s_2 & -L_2 c_2 \\ L_2 c_2 & L_1 + L_2 s_2 \end{bmatrix} = \left(L_1 + L_2 s_2\right)^2 + \left(L_2 s_2\right)^2 \quad (16)$$

$$\Delta s_1 = \begin{bmatrix} L_1 + L_2 s_2 & -p_x \\ L_2 c_2 & -p_y \end{bmatrix} = \left(L_1 + L_2 s_2\right)p_y - \left(L_2 c_2\right)p_x \quad (17)$$

$$\Delta c_1 = \begin{bmatrix} p_x & -L_2 s_2 \\ p_y & L_1 + L_2 c_2 \end{bmatrix} = \left(L_1 + L_2 c_2\right)p_x + \left(L_2 s_2\right)p_y \quad (18)$$


Published By:
Blue Eyes Intelligence Engineering
and Sciences Publication (BEIESP)

$$c_1 = \frac{\Delta c_1}{\Delta} = \frac{(L_1 + L_2 s_2)p_y - L_2 c_2 p_x}{(L_1 + L_2 s_2)^2 + (L_2 c_2)^2} = \frac{(L_1 + L_2 s_2)p_y - L_2 c_2 p_x}{p_x^2 + p_y^2} \quad (19)$$

$$s_1 = \frac{\Delta s_1}{\Delta} = \frac{(L_1 + L_2 s_2)p_x - L_2 c_2 p_y}{(L_1 + L_2 s_2)^2 + (L_2 c_2)^2} = \frac{(L_1 + L_2 s_2)p_x - L_2 c_2 p_y}{p_x^2 + p_y^2} \quad (20)$$

$$\theta_1 = \tan^{-1}\frac{s_1}{c_1} = \tan^{-1}\frac{(L_1 + L_2 c_2)p_y - L_2 s_2 p_x}{(L_1 + L_2 c_2)p_x - L_2 s_2 p_y} \quad (21)$$

By comparing elements 4,4 from equation (5) and (6):

$$d_3 = -p_z - d_4 \quad (22)$$

Then

$$\theta_3 = 0 \quad (23)$$

By comparing elements 1,1 and 2,1 from equation (4) and (8):

$$s_4 = n_x s_{12} + n_y c_{12} \quad (24)$$

$$c_4 = -n_x c_{12} + n_y s_{12} \quad (25)$$

$$\theta_4 = \tan^{-1}\frac{-n_x \sin(\theta_1 + \theta_2) + n_y \cos(\theta_1 + \theta_2)}{n_x \cos(\theta_1 + \theta_2) + n_y \sin(\theta_1 + \theta_2)} \quad (26)$$

**b) Velocity Inverse**

Inverse equation (10) and equation (11)

$$\dot{p}_x = -L_1 c_1 \dot{\theta}_1 - L_2 c_{12}(\dot{\theta}_1 + \dot{\theta}_2) \quad (27)$$

$$\dot{p}_y = +L_1 s_1 \dot{\theta}_1 - L_2 s_{12}(\dot{\theta}_1 + \dot{\theta}_2) \quad (28)$$

So,

$$\dot{p}_x = -(L_1 c_1 + L_2)\dot{\theta}_1 - L_2 c_{12}\dot{\theta}_2 \quad (29)$$

$$\dot{p}_y = -(L_1 s_1 + L_2 c_{12})\dot{\theta}_1 + L_2 c_{12}\dot{\theta}_2 \quad (30)$$

By solving equation (31) and equation (32) (Kramer's rule)

$$\dot{\theta}_1 = \frac{\dot{p}_x s_{12} + \dot{p}_y c_{12}}{L_1 c_2} \quad (31)$$

$$\dot{\theta}_2 = \frac{-\dot{p}_y(L_1 c_1 + L_2 c_{12}) - -\dot{p}_x(L_1 s_1 + L_2 s_{12})}{L_1 L_2 c_2} \quad (32)$$

Translational velocity:

$$\dot{d}_3 = -\dot{p}_z \quad (33)$$

Differentiating the equation (26):

$$s_4 d\theta_4 = -[dn_x c_{12}(d\theta_1 + d\theta_2)] + d_{ny} s_{12} - n_y c_{12}(d\theta_1 + d\theta_2) \quad (34)$$

So,

$$d\theta_4 = -\frac{d\theta_1 + d\theta_2}{s_4}(n_x s_{12} + n_y c_{12}) - \frac{c_{12}}{s_4} dn_x + \frac{s_{12}}{s_4} dn_y \quad (35)$$

Then,

$$\dot{\theta}_4 = \frac{d\theta}{dt} = \frac{s_{12}\dot{n} - c_{12}\dot{n}_x - (n_x s_{12} + n_y c_{12})\dot{\theta}_{12}}{s_4} \quad (36)$$

**c) Acceleration Inverse**

$$\ddot{\theta}_1 = \frac{-(\dot{p}_x c_{12} + \dot{p}_y s_{12})\dot{\theta}_{12} + (\ddot{p}_x s_{12} + \ddot{p}_y c_{12}) - L_1 s_2 \dot{\theta}_1 \dot{\theta}_2}{L_1 c_1} \quad (37)$$


Published By:
Blue Eyes Intelligence Engineering
and Sciences Publication (BEIESP)

$$\ddot{\theta}_2 = \frac{\left[(\ddot{p}_x c_1 - \ddot{p}_x s_1)L_1 + (\ddot{p}_x c_{12} - \ddot{p}_x s_{12})L_2 + (\dot{p}_y s_1 - \dot{p}_x c_1)L_1\dot{\theta}_1 + (\dot{p}_y s_{12} + \dot{p}_x c_{12})L_2\dot{\theta}_{12} + L_1 L_2\dot{\theta}_2^2\right]}{L_1 L_2 c_2} \quad (38)$$

$$\ddot{d}_3 = -\ddot{p}_x \quad (39)$$

$$\ddot{\theta}_4 = \frac{\ddot{n}_y s_{12} - \ddot{n}_x c_{12} - (2\dot{n}_y c_{12} + 2\dot{n}_x s_{12})\ddot{\theta}_{12} - (n_y s_{12} - n_x c_{12})\dot{\theta}_{12}^2 - (n_x s_{12} + n_y c_{12})\ddot{\theta}_{12} + c_4\dot{\theta}_4^2}{s_4} \quad (40)$$

**2.2 Robot Dynamics**

Form figure 3, the torques at each joints are [20,21]:

$$T_1 = b_{11}\ddot{\theta}_1 - b_{12}\ddot{\theta}_1 - b_{13}d_3 - b_{14}\dot{\theta}_1\dot{\theta}_2 + b_{15}\dot{\theta}_2^2 \quad (41)$$

$$T_2 = b_{21}\ddot{\theta}_1 + b_{22}\ddot{\theta}_2 + b_{23}\ddot{d}_3 + b_{24}\dot{\theta}_2^2 \quad (42)$$

$$T_3 = -b_{31}\ddot{\theta}_1 + b_{32}\ddot{\theta}_2 + b_{33}\ddot{d}_3 - b_{34} \quad (43)$$

Where:

$$b_{11} = r_1^2 m_1 + j_1 + g_{r1}^2 j_{m1} + (L_1^2 + r_2^2 + 2L_1 r_2 c_2)m_2 + L_1^2 m_{m2} + j_2 + j_{m2} +$$
$$(L_1^2 + L_2^2 + 2L_1 L_2 c_2)(m_3 + m_{m3}) + j_3 + j_{m3}$$

$$b_{12} = (r_2^2 + L_1 r_2 s_2)m_2 + j_2 + g_{r2} j_{m2} + (L_1^2 + L_1 L_2 s_2)(m_3 + m_{m3}) + j_3 + j_{m2}$$

$$b_{13} = g_{r3} j_{m3} \; ; \quad b_{14} = 2L_1 c_2[m_2 r_2 + (m_3 + m_{m3})L_2]$$

$$b_{15} = L_1 c_2[m_2 r_2 + (m_3 + m_{m3})L_2] \; ; \quad b_{15} = L_1 c_2[m_2 r_2 + (m_3 + m_{m3})L_2]$$

$$b_{21} = m_2(r_2^2 + L_1 r_2 s_2) + j_2 + g_{r2} j_{m2} + (L_1^2 + L_1 L_2 s_2)(m_3 + m_{m3}) + j_3 + j_{m3}$$

$$b_{22} = r_2^2 m_2 + j_2 + g_{r2}^2 j_{m2} + L_2^2(m_3 + m_{m3}) + j_3 + j_{m3}$$

$$b_{23} = g_{r3} j_{m3} \; ; \quad b_{24} = L_1 c_2[m_2 r_2(m_3 + m_{m3})L_2]$$

$$b_{31} = b_{32} = g_{r3} j_{m3} \; ; \quad b_{33} = m_3 + g_{r3} j_{m3} \; ; \quad b_{34} = m_3 g$$

**2.3 Actuator Modeling**

Actuator is a responsible device for mobiling or moving robots. motors (DC, stepper) and pistons (pneumatic, hydraulic) are remarkable kinds of this divice. This research presents the comlete as well as detailed procdure through using this actuator model type using Dc motor. The motor drive utilized PWM control in order to manage the voltage supply, , that uses microcontrollers for these followig gains;

1) their lightness and size
2) less inputs and outputs
3) Remote process
4) Armature unsettled voltage with least waste (loss)

The separate-wound motor equations leading permanent-magnet operation at constant flux as below [22,23]:

$$V_a = Ri_a + e_a + L\frac{di_a}{dt} \quad (44)$$

$$e_a = k_\omega \omega_m \quad (45)$$

$$T = k_e \phi i_a = k_T i_\omega \quad (46)$$

$$T = T_L + j_m\frac{d\omega_m}{dt} + b\omega_m \quad (47)$$

**2.4 Transmission Model**

mechanical power elements including load, actuator and Gear which are the most well-known are the switch model in a robot convey. The most well-known robotic revolute-joint transmission element which has a extremely high transmission ratio is harmonic drive. The usage of the transmitted torque shaft (T) and inertia could be specified [24,25].

$$T = T_L / g_r\eta \Rightarrow T\frac{\omega_m}{\omega_L}\eta = T\frac{\theta_m}{\theta_L}\eta = T_L \quad (48)$$

$$J = j_m + J_L / g_r^2 \quad (49)$$

For linear velocity at third joint can be caluated as:

$$\omega_m = \frac{D}{2} = \dot{d}_3 \quad (50)$$

**2.5 Adaptive Neuro Fuzzy Inference Scheme (ANFIS)**

This section presents a brief background description of ANFIS which is used of controlling parameters of Plant's system. The Neural network (NN) paradigm is inspired from human thought and has been used in many applications successfully such as constructing software agents or autonomous robots and controlling machines, image analysis, adaptive control and voice recognition.


Published By:
Blue Eyes Intelligence Engineering
and Sciences Publication (BEIESP)

NNs can be used to identify dynamic systems control which projected in the field of electronics and AC drives because of its characteristics such as high fault tolerance and in term of speed estimation its fast parallel computation. To getting better performance of NN paradigm it can be trained with different patterns like integrating Fuzzy logic (FL) with neural network to control different parameters of real-time systems [26-29].

## III. ANFIS CONTROLLER DESIGN

System operations can be controlled through the decisions it makes by a controller. A control system brings stability during disturbances, safeguarding from equipment damages. It may be hardware-based, software-based, or both. This section develops an ANFIS control scheme as shown in Fig. 1, for SCARA robot parameters such as speed, accuracy, envelop and high performance. Fuzzy set is an extension of a 'crisp' set where an element belongs to either a set (full membership) or to none (no membership). Fuzzy sets allow partial membership, i.e., membership to more than one set [24-28].

**Fig. 1: The ANFIS control scheme for speed control of the IM [2,30-32]**

A fuzzy set A of a universe of discourse X is represented by a collection of ordered pairs of generic element and its membership function μ : X → [ 0 1], which associates a number μA(x) : X → [ 0 1] to each element x of X. An FLC uses a set of control rules called fuzzy rules, expressed among the linguistic variables as conditional statements. The basic structure of this work's ANFIS controller comprises 4 blocks: fuzzification, knowledge base, neural network, and de-fuzzification; each will be explained briefly in the next paragraphs. The inputs to the ANFIS controller, i.e., the error and the change in error, are modelled through Eqn. (50) as

$$\left.\begin{aligned} e(k) &= \omega_{ref} - \omega_r \\ \Delta e(k) &= e(k) - e(k-1) \end{aligned}\right\} \quad (50)$$

Where $w_{ref}$ is the reference speed, $w_r$ the actual rotor speed, e(k) the error, and Δe(k) the change in error. The fuzzification unit converts the crisp data into linguistic variables, given as inputs to the rule-based block. The set of 49 rules are based on past knowledge/experiences in the rule-based block, which connects to the NN block. Back propagation algorithm trains the NN to select the proper set of rule base. In developing the control signal, the training is very important for selection of the proper rule base. Selection, and then firing of the proper rules, generates the control signal needed for optimal outputs. The output of the NN unit is given as input to the de-fuzzification unit and the linguistic variables are re-converted into numeric data, as crisps. In fuzzification, the crisp variables, the speed error, and the change in error are converted into fuzzy variables or linguistics variables. The fuzzification maps the 2 input variables to linguistic labels of the fuzzy sets. The fuzzy coordinated controller uses the linguistic labels. Each fuzzy label has an associated MF. Triangular MF was used here (see Fig. 2-a,b). The inputs are fuzzified through the fuzzy sets and given as input to the ANFIS controller. Table 2 lists the rule base for selection of the proper rules through back propagation algorithm.

**Table 2: The rule base for speed control**

| ΔE\E | NB | NM | NS | ZE | PS | PM | PB |
|---|---|---|---|---|---|---|---|
| NB | NB | NB | NB | NB | NM | NS | ZE |
| NM | NB | NB | NM | NM | NS | ZE | PS |
| NS | NB | NM | NS | NS | ZE | PS | PM |
| ZE | NB | NM | NS | ZE | PS | PM | PB |
| PS | NM | NS | ZE | PS | PS | PM | PB |
| PM | NS | ZE | PS | PM | PM | PB | PB |
| PB | ZE | PS | PM | PB | PB | PB | PB |


Published By:
Blue Eyes Intelligence Engineering
and Sciences Publication (BEIESP)

Table 2, the control decisions are based on the fuzzified variables. The inference uses a set of rules in determining the output decisions. As there are 2 input variables and 7 fuzzified variables, the controller has a set of 49 rules for the ANFIS controller. From the 49 rules [Fig. 2-c,d], the proper rules are selected by NN training helped by RBFNN algorithm, before the selected rules are fired. Further, it has to be converted into numerical output, i.e., they have to be de-fuzzified. This process is defuzzification, which produces a quantifiable result in FL. Defuzzification transforms fuzzy set information into numeric data information. Methods of defuzzification include centre of gravity, centre of singleton, maximum, marginal properties of centroid, etc. This work used the centre-of-gravity method. The output of the defuzzification unit generates the control commands that are given as input (crisp input), through the inverter, to the plant. Any deviation in the controlled output is feedback and compared with the set value and the error signal generated, and given as input to the ANFIS controller, which restores the output to the normal value, maintaining system stability. Eqn. (51) gives the controlled output signal y, which is the controller's final output and is the weighted average of the proper rule-based outputs selected by the back-propagation algorithm.

$$y = \left( \sum_{i=1}^{R} \mu^i a_1^i x_1 \right) + \Lambda + \sum_{i=1}^{R} \mu^i a_q^i x_q \Big/ \sum_{i=1}^{R} \mu^i \qquad (51)$$

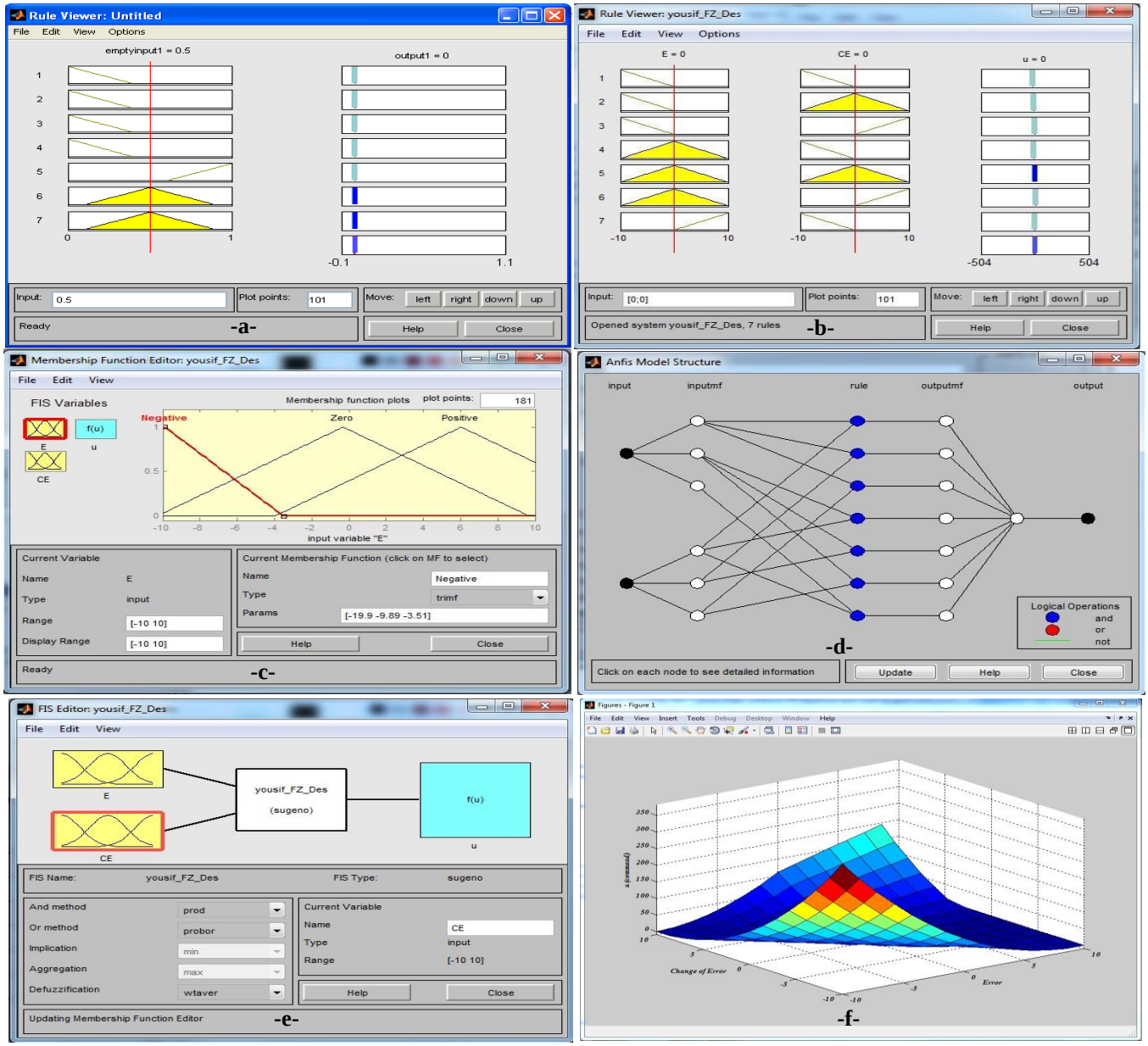


**Fig. 2 (a-f). Learning and analysis of the ANFIS controller**


*Published By:*
*Blue Eyes Intelligence Engineering and Sciences Publication (BEIESP)*

## IV. SCARA ROBOT VIRTUAL REALITY

The requirements for design in VRML are explained in *finite processing allocations*, *autonomy*, *consistent self-registration* and *calculability*. Design in VRML depends on the designer's information and his imagination of the object. VR design choices are standard configurations (sphere, cone, cylinder, etc.) and free-form (the indexed face set button is selected, to get many configurations with points that can be rearranged). Every real-form design is considered free-form designing, which starts with building parts one by one and checking the shape against a related, real manipulator part. That robot part cannot be simulated in VR when the standard shape from the VR library is used, where they are not uniform shape. The design uses the indexed face set in VR.

The next design step is connecting all the parts to produce the object and to limit the object's point of origin. This job was made by setting the first shape (e.g. the base) and then connecting the next shape (joint two) in the "children" button; the same procedure is repeated with other parts. Fig. 3 is the design, in full VR, of a SCARA robot with vacuum handling wrist.


**Fig.3. A SCARA robot left arm, in VR view through Matlab**

## V. RESULTS AND DISCUSSION

Fig. 3 VR model using Matlab Simulink R2012a for the neuro-fuzzy controller tracking the SCARA trajectory. Starting off the simulations is the invoking of the 49-fuzzy-rule set from the Matlab command window; the fuzzy file where the rules are written with T-S control strategy incorporated is opened, then the fuzzy editor (FIS) dialogue box opens. The .fis file (yousif_FZ_Des) is imported through the command window from the source, and then opened (through file-open command) in the fuzzy editor dialog box. Figs. 2 a-f shows opening of the file activating the TS fuzzy-rule file. The data is exported to the workspace, and the simulations are run for e.g., 60s.

The fuzzy MF editor is next obtained from the menu bar, through view membership command (see Figs. 2 a-b). The rule-view command enables viewing of the TS-fuzzy rules written. It is the pictorial rule viewer for the 2 inputs and 1 output. Post preliminary operations, the VR model is called up through the interface block between it and Matlab. Fig. 2e shows the ANFIS editor opening in the command window. The workspace-data variables are loaded onto the ANFIS editor (see Figs. 2 a-f). The .fis file is next generated in the ANFIS editor through loading of the workspace data. Once the .fis file is generated, the ANFIS has to be trained properly through a proper algorithm with enough epochs. In rule-training, this work used back-propagation algorithm with an appropriate number of epochs. The 2 items are selected in the train window of the ANFIS editor, and the NN is trained for proper-rule-base selection. Next the trained data is exported to the workspace, through file-export command. Fig. (2.f) is the surface plot for error signal and the change in output error.


Published By:
Blue Eyes Intelligence Engineering
and Sciences Publication (BEIESP)

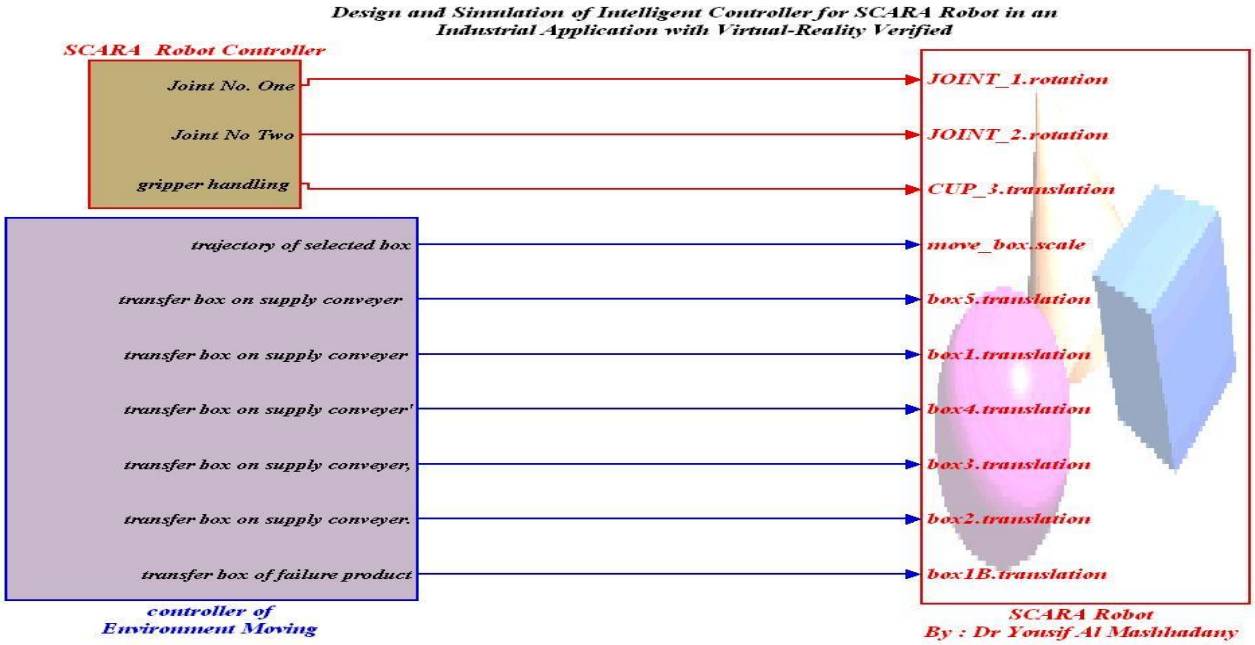


**Fig. 4. Simulation of the Intelligent Controller for the Virtual-Reality-Verified Industrial-Application SCARA Robot**

The ANFIS controller designed trained the NN through the fuzzy-rule base, to select the proper and optimal rule. The hidden layers use 7x7 rules. Neuron-1 connects to 7 fuzzy rules, as does Neuron-2. The hidden layers have 49-49 neurons selecting the proper rule base. The 49 fuzzy rules are fired, de-fuzzified output obtained as output neuron. Through the value of the calculated command, the de-fuzzified output generates the firing pulse to be applied to the actuator of each motor joint. Post-simulation, the performance of the SCARA is evaluated through its movements, which are recordable in video or photograph and observable according to scope.

The control system with intelligent controller for the industrial-application SCARA, with the joints connected, in VR modeling (see Fig. 3), was simulated by using Matlab R2014a. The results prove the effectiveness of the proposed neuro-fuzzy controller. The highly accurate model of the system shows the drive speeding up with faster dynamism. The response characteristics curve of the proposed neuro-fuzzy controller shows, as compared with work in [2, 10, 20, and 30], faster settling and reaching of steady state. Figs. (5 a-d) shows the robot trajectory in a factory application of quality-control defect screening. Defective items are selected by an electro photo sensor with a weight measurement sensor that limits failure in weighing the pieces in the production line. Compared with other methods, the ANFIS control achieves system stability faster through the ANN training and use of the proper rule-base. The desired trajectory is accurately achieved through accurate positioning and orientation of the end-effector (see Figs. 5 a-d).

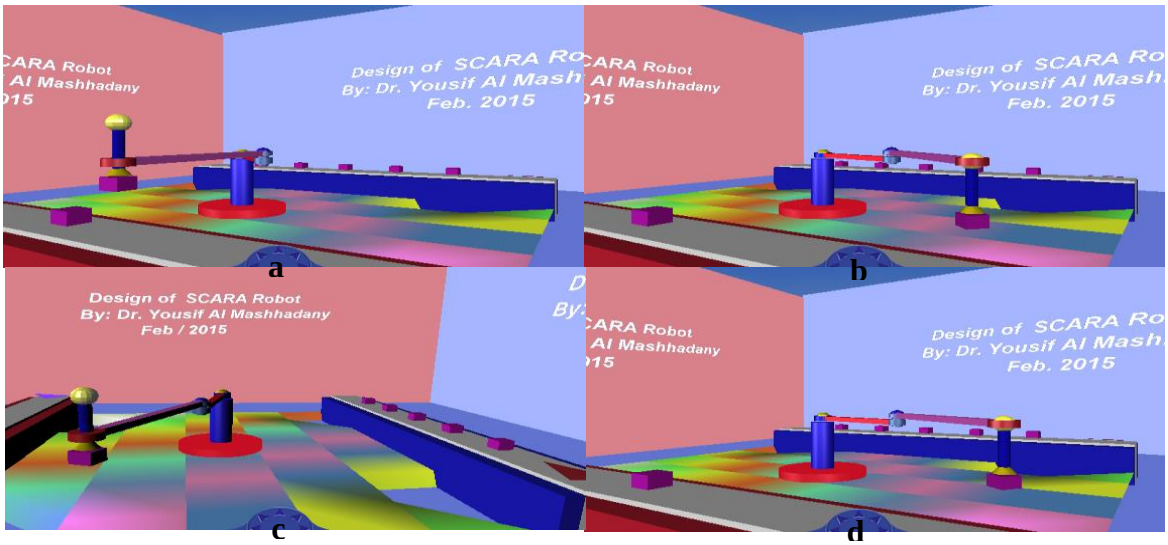


**Fig. 5 (a-d): Movements of the SCARA in production-line screening**


Published By:
Blue Eyes Intelligence Engineering
and Sciences Publication (BEIESP)

Fig.6 shows the rotation signal of the SCARA joints and translation of the gripper movements through a sixty-second delivery-period simulation test. The SCARA very accurately detects defective items as signaled by the photoelectric sensor before transferring them to another conveyor, which returns them. The SCARA moves five defective pieces per minute.

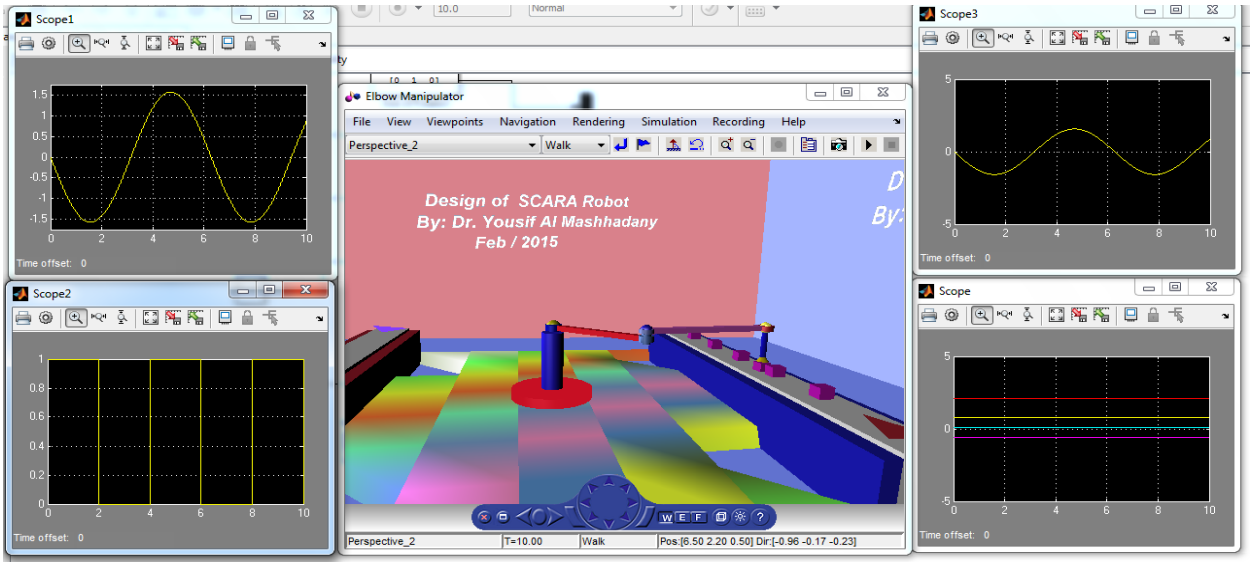


**Fig. 6. Controlled signal for movement robot joints and environment**

## VI. CONCLUSIONS

The accurate results of the simulation are providing the ability of implement the system design of SCARA with ANFIS controller. ANFIS has effective computation and works well with linear, optimization, and adaptive techniques. Compared with other control strategies, it operates much faster. The ANFIS controller developed here settles and stabilizes quickly and has very good dynamic response. The use of photoelectric sensor as sensing element in the control system increased effectiveness. This sensor has sufficient real specification for its practical implementation in the control system proposed.

## ACKNOWLEDGEMENT

Special thanks from authors to Ishik University for supporting this work.

## REFERENCES

[1] M. Isaksson, T. Brogårdh, M. Watson, S. Nahavandi, P. Crothers, The Octahedral Hexarot A novel 6-DOF parallel manipulator, Journal of Mechanism and Machine Theory, Vol. 55, pp. 91–102, 2012
[2] Y. Al Mashhadany, "Design, Analysis, Simulation, and Virtual-Reality-Verified Intelligent Controller for Industrial-Application SCARA Robot", International Journal of Advanced Computing, June, 2013
[3] F. Bravo, G. Carbone, J. Fortes, Collision free trajectory planning for hybrid manipulators, journal of mechatronics, http://dx.doi.org/10.1016/j.mechatronics.2012.05.001, 2012.
[4] A. Djuric, R. AlSaidi,W. ElMaraghy , "Dynamics solution of n-DOF global machinery model, Journal of Robotics and Computer-Inegrated Manufacturing, Vol. 28, pp. 621– 630, 2012
[5] S. Toroghia , M. Gharibb, A. Ramezanic, K. Rahmdelb, Modeling and Robust Controller Design for an Industrial Boiler, 2011 2nd International Conference on Advances in Energy Engineering, Journal Energy Procedia, Vol. 14, pp. 1471-1477, 2011
[6] T.Benjanarasuth, N. Sowannee, N. Naksuk, "Two-Degree-of-Freedom Simple Servo Adaptive Control for SCARA Robot", International Conference on Control, Automation and Systems, Oct. 27-30, in KINTEX, Gyeonggi-do, Korea, pp. 489 – 484, 2010
[7] M.Liyanage, N. Krouglicof , R. Gosine, "Development and Testing of a Novel High Speed SCARA Type Manipulator For Robotic Applications", IEEE International Conference on Robotics and Automation Shanghai International Conference Center , May 9-13,Shanghai, China, pp. 3226 – 3242, 2011
[8] A. Nagchaudhuri, "Experience with Introducing Robotics Toolbox for MATLAB in a Senior Level Undergraduate Course" ASME International Mechanical Engineering Congress and Exposition November 13-19, Lake Buena Vista, Florida, USA, pp. 1-8, 2009
[9] S. B. Shamsulkamar, " Modeling And Control Of 6-Dof Of Industrial Robot By Using Neuro-Fuzzy Controller", MSc thesis Universiti Tun Hussein On Malaysia, Jan. 2014
[10] Y. Al Mashhadany, " Hybrid ANFIS Controller for 6-DOF Manipulator with 3D Model", International Journal of Computers & Technology, Vol. 4, No. 2, ISSN 2277-3061, www.cirworld.com, April, 2013.
[11] M. Short, K. Burn, A generic controller architecture for intelligent robotic systems, Journal of Robotics and Computer-Integrated Manufacturing, Vol. 27, No.2, pp. 292–305, 2011.
[12] Y. Al Mashhadany, "Advance 6-DOF Manipulator Controller Design Using DMRAC Based ANFIS" , Wulfenia Journal, Austria, ISNN: 1561-882X, Vol 20, No. 3;Mar 2013.
[13] H. Souley Ali, L. Boutat-Baddas, Y. Becis-Aubry and M. Darouach," H∞ control of a SCARA robot using polytopic LPV approach" 14th Mediterranean Conference on Control and Automation, MED '06,pp. 1 - 5,2006.
[14] J. Antonio, J. de Lope, M. Santos, A method to learn the inverse kinematics of multi-link robots by evolving neuro-controllers Journal of Neurocomputing, Vol. 72, No.13–15, pp. 2806–2814, 2009.
[15] M. Taylan Das, L. Canajournal on Dulger, Mathematical modeling, simulation and experimental verification of a scara robot, Journal of Simulation Modelling Practice and Theory, Vol.13, No.3, pp. 257–271, 2005.
[16] F.Bravoa, G. Carboneb, J.C. Fortes, Collision free trajectory planning for hybrid manipulators, Journal of Mechatronics, In Press, 2012.
[17] P. Cheng, K. Cheng, Evaluation of the dynamic performance variation of a serial manipulator after eliminating the self-weight influence, journal of Mechatronics, Vol.21, No.6, pp. 993–1002, 2011.
[18] A. Medjebouri, L. Mehennaoui," Active Disturbance Rejection Control of a SCARA Robot Arm", International Journal of u- and e-Service, Science and Technology Vol.8, No.1, pp.435-446, 2015
[19] Z.Liang, S.Meng, D.Changkun," Accuracy Analysis of SCARA Industrial Robot Based on Screw Theory" IEEE International Conference on Computer Science and Automation Engineering (CSAE), Vol.3, pp.40-46, 2011.
[20] Y. I. Al Mashhadany, S. Adel, A. Abdu sattar, A. Khuder, "Novel Controller for PUMA 560 Based on PIC Microcontroller", has been accepted for publication in Wulfenia Journal, Vol. 21, Iss. 4, 2014


Published By:
Blue Eyes Intelligence Engineering
and Sciences Publication (BEIESP)

[21] M. Nkomo, M. Collier, “A Color-Sorting SCARA Robotic Arm”, 2nd International Conference on Consumer Electronics, Communications and Networks (CECNet), pp. 763 - 768, 20012.
[22] S.Takagi, N. Uchiyama, Robust Control System Design for SCARA Robots Using Adaptive Pole Placement, IEEE Transaction on Industrial Electronics, Vol. 52, No. 3, pp.915-921,2005.
[23] Sahin, Y., Ankarali, A.; Tinkir, M.,” Neuro-Fuzzy trajectory control of a scara robot” IEEE 2nd International Conference on Computer and Automation Engineering (ICCAE), pp. 298- 302, 2010.
[24] R.Rodriguez, A. Cedeno , U.Costa , J. Solana, C. Caceres, E.Opisso , J.M. Tormos , J. Medina , E. J. Gomez, Inverse kinematics of a 6 DoF human upper limb using ANFIS and ANN for anticipatory actuation in ADL-based physical Neurore habilitation, Journal of Expert Systems with Applications ,Vol.39, No.10.
[25] S.Volker, Optmized SCARA kinematic description and examples, International Symposium on Robotics (ISR), 2010 41st and 2010 6th German Conference on Robotics (ROBOTIK), pp.1-5, 2010.
[26] S.Yamacli , H.Canbolat, Simulation of a SCARA robot with PD and learning controllers, Journal of Simulation Modeling Practice and Theory, Volume 16, Issue 9,pp. 1477–1487,2008.
[27] M. Isaksson, T. Brogardh, I. Lundberg, S.Nahavandi, “Improving the Kinematic Performance of the SCARA-Tau PKM” IEEE International Conference on Robotics and Automation, pp. 4683-4690,2010.
[28] S. Majidabad, A. Kalat, H. Shandiz” Neuro-Fuzzy-Discrete Sliding Mode Control of a Tree-Link SCARA Robot” 19th Iranian Conference on Electrical Engineering (ICEE),pp.1, 2011 .
[29] A. L. Talli, B. B. Kottursheṭtar, " Kinematic Analysis, Simulation & Workspace Tracing of Anthropomorphic Robot Manipulator By Using MSC. ADAMS", International Journal of Innovative Research in Science, Engineering and Technology Vol. 4, Issue 1, January 2015
[30] Y. Al Mashhadany,"High-Performance of Power System Based upon ANFIS (Adaptive Neuro-Fuzzy Inference System) Controller", Journal of Energy and Power Engineering 8 , 729-734, 2014.
[31] M. Joo, M. T. Lim, H. S. Lim, Real-time hybrid adaptive fuzzy control of a SCARA robot, Journal of Microprocessors and Microsystems, Vol.25, No.8, pp. 369–378, 2001.
[32] M. Plius, M. Yilmaz, U. Seven and K. Erbatur” Fuzzy Controller Scheduling for Robotic Manipulator Force Control, 12th IEEE International Workshop on Advanced Motion Control, pp.1-8, 2012.


*Published By:*
*Blue Eyes Intelligence Engineering and Sciences Publication (BEIESP)*